



Ultraviolet Flux Decrease Under a Grand Minimum from *IUE* Short-wavelength Observation of Solar Analogs

Dan Lubin¹, Carl Melis² , and David Tytler²

¹ Scripps Institution of Oceanography, University of California, San Diego, 9500 Gilman Drive, La Jolla, CA 92093-0221, USA; dlubin@ucsd.edu

² Center for Astrophysics and Space Science, University of California, San Diego, 9500 Gilman Drive, La Jolla, CA 92093-0424, USA

Received 2017 September 1; revised 2017 November 30; accepted 2017 December 11; published 2017 December 27

Abstract

We have identified a sample of 33 Sun-like stars observed by the *International Ultraviolet Explorer* (*IUE*) with the short-wavelength spectrographs that have ground-based detections of chromospheric Ca II H+K activity. Our objective is to determine if these observations can provide an estimate of the decrease in ultraviolet (UV) surface flux associated with a transition from a normal stellar cycle to a grand-minimum state. The activity detections, corrected to solar metallicity, span the range $-5.16 < \log R'_{HK} < -4.26$, and eight stars have $\log R'_{HK} < -5.00$. The *IUE*-observed flux spectra are integrated over the wavelength range 1250–1910 Å, transformed to surface fluxes, and then normalized to solar $B - V$. These normalized surface fluxes show a strong linear relationship with activity R'_{HK} ($R^2 = 0.857$ after three outliers are omitted). From this linear regression we estimate a range in UV flux of 9.3% over solar cycle 22 and a reduction of 6.9% below solar cycle minimum under a grand minimum. The 95% confidence interval in this grand-minimum estimate is 5.5%–8.4%. An alternative estimate is provided by the *IUE* observations of τ Cet (HD 10700), a star having strong evidence of being in a grand-minimum state, and this star's normalized surface flux is $23.0 \pm 5.7\%$ lower than solar cycle minimum.

Key words: stars: activity – stars: solar-type – Sun: activity – Sun: UV radiation – ultraviolet: stars

1. Introduction

Over the past decade there has been increasing realization and concern that the steady and high solar luminosity of the past century may transition to greater variability later this century (Abreu et al. 2008; Feulner & Rahmstorf 2010; Lockwood 2010). Specifically, the Sun may descend into a period of low magnetic activity analogous to the historical Maunder minimum (MM; circa 1640–1715; Eddy 1976). A resulting decrease in total solar irradiance (TSI) impacting the terrestrial lower atmosphere energy budget is linked to changes in high-latitude circulation patterns that strongly influence the climate of Europe and the Atlantic sector of the Arctic and sub-Arctic (Song et al. 2010; Meehl et al. 2013), and may also influence Antarctic climate (Orsi et al. 2012). Studies have also shown the importance of stratospheric response to a grand minimum (e.g., Gray et al. 2010; Bolduc et al. 2015; Maycock et al. 2015). Over a solar cycle and certainly in response to a future grand minimum, irradiance variability at middle ultraviolet (UV) wavelengths that drive oxygen photolysis and ozone chemistry is much larger than that of the TSI. Resulting changes to stratospheric ozone abundance alter the stratosphere–troposphere temperature gradient and feed back to tropospheric planetary wave refraction, further altering climatically relevant circulation patterns (Maycock et al. 2015). With this realization that both direct radiative and indirect stratospheric influences affect terrestrial climate under a solar grand minimum, it is important to understand how UV irradiance would respond to such a large and prolonged change in solar magnetic activity.

Spectral UV irradiance during the historical MM is usually inferred from time series reconstructions grounded by the distribution of solar surface features over the course of current cycles or by geophysical proxies (e.g., Lean 2000; Krivova et al. 2010; Shapiro et al. 2011; Bolduc et al. 2014). Solar analogs have mainly been employed to make individual stellar

comparisons with the Sun (e.g., Judge et al. 2004), or in surveys to estimate the percentage of very low activity stars occurring in the local field population as an indicator of how frequently grand minima occur throughout the Sun's lifetime (e.g., Baliunas & Jastrow 1990; Henry et al. 1996; Hall & Lockwood 2004; Wright et al. 2004; Lubin et al. 2012; Curtis 2017). In this study, we explore whether an aggregate sample of *International Ultraviolet Explorer* (*IUE*) observations of Sun-like stars, acquired for multiple unrelated observing programs between 1978 and 1996 and maintained as archival data, can be used to estimate the decrease in UV flux associated with a grand minimum.

2. Data

Solar analogs were selected from the *IUE* MAST archive for which there is at least one observation of Ca II H+K chromospheric activity reported in the literature and at least one useful *IUE* short-wavelength (SW) spectrum (most stars have multiple spectra). All *IUE* spectra considered here were obtained at low resolution (~ 6 Å). In individual SW spectra, an absolute calibration uncertainty of 5% is an appropriate estimate (Bohlin 1986). However, in this work we must also consider dispersion between individual spectra obtained from stars with varying magnitudes. Table 1 of Bohlin et al. (1990) gives examples for *IUE* SW data. In these examples dispersions are of the order of 4%–5% for hot stars with strong UV flux, but become larger for nearby G stars (8.9% for β Hyi) and even larger still (35%–58%) for fainter G stars. We therefore expect there might be large variance among spectra for some stars. To evaluate uncertainty in the averaged fluxes for each solar analog, we use the standard deviation of the wavelength-integrated fluxes for stars with multiple spectra. For stars with just one spectrum we adopt a standard deviation of 9% based on Bohlin et al. (1990).

Table 1
IUE SW Solar Analogs

HIP	HD	$B - V$	T_e (K)	$\langle [\text{Fe}/\text{H}] \rangle$	$\langle \log R'_{HK} \rangle$	R'_{HK} source	F_s	$\sigma(F_s)$	$\log g$
	Sun	0.656	5777	0.000	-4.822	2	2.462		
	Sun	0.656	5777	0.000	-4.951	2	2.234		
1599	1581	0.576	5929	-0.232	-4.911	3, 11	7.763	0.223	4.51(1), 4.46(2)
1803	1835	0.659	5689	0.177	-4.412	1-3, 7	4.762	0.357	4.44(1), 4.47(2)
4290	5294	0.652	5728	-0.210	-4.536	1, 9	3.301	0.297	4.48(3)
8102	10700	0.727	5420	-0.539	-5.031	1-3, 5, 7, 9-11	1.049	0.060	4.31(1), 4.59(2)
15330	20766	0.641	5702	-0.208	-4.667	3, 5	3.923	0.353	4.39(1), 4.58(2)
15371	20807	0.600	5835	-0.206	-4.858	3, 11	5.504	0.495	4.43(1), 4.54(2)
15457	20630	0.681	5702	0.007	-4.419	1, 2, 9	3.931	0.182	4.40(1), 4.49(2)
15510	20794	0.711	5458	-0.394	-5.024	3, 11	1.200	0.132	4.30(1), 4.62(2)
24813	34411	0.630	5875	-0.002	-5.066	1, 6, 7, 9	4.243	0.382	4.16(1), 4.37(2)
27913	39587	0.594	5902	-0.025	-4.428	1, 6, 9	9.288	0.422	4.39(1), 4.34(2)
30104	44594	0.657	5754	0.130	-4.946	3, 11	3.057	0.275	4.43(1), 4.41(2)
33719	52265	0.572	6081	0.210	-5.046	7, 9	9.655	0.869	4.29(1), 4.26(2)
37853	63077	0.589	5794	-0.884	-5.019	3, 7	8.438	3.559	4.01(1)
42291	73524	0.598	5902	0.075	-4.989	3, 11	5.335	0.480	4.32(1), 4.41(2)
43726	76151	0.661	5676	0.034	-4.647	1-3	2.649	0.238	4.41(1), 4.55(2)
44897	78366	0.585	5916	0.080	-4.570	1, 2, 6, 9	7.607	1.327	4.54(2)
47592	84117	0.534	6138	-0.070	-5.036	9	16.156	0.501	4.31(2)
51248	90508	0.610	5728	-0.330	-5.013	1, 6	2.247	0.202	4.35(1)
53721	95128	0.624	5834	-0.014	-4.990	1, 7	4.149	0.374	4.24(1), 4.38(2)
56997	101501	0.723	5483	0.030	-4.565	2, 6, 7	1.881	0.119	4.69(1), 4.43(2)
57443	102365	0.664	5649	-0.330	-4.973	3, 9	2.619	0.179	4.32(1), 4.57(2)
64394	114710	0.572	5970	0.014	-4.739	1, 2, 7, 9	6.311	2.697	4.34(1), 4.57(2)
64792	115383	0.585	5957	0.075	-4.408	1-3, 7, 9	11.253	0.551	4.11(1), 4.60(2)
64924	115617	0.709	5572	-0.028	-5.004	1-3, 7, 9, 11	1.509	0.136	4.27(1), 4.47(2)
72659	131156	0.720	5570	0.020	-4.348	1-3, 6, 7	2.479	0.110	4.60(1), 4.65(2)
75676	138004	0.676	5888	-0.470	-4.900	6, 7, 9	2.256	0.203	4.49(2)
77257	141004	0.604	5888	-0.022	-4.987	1-3, 6, 7, 9	5.285	0.199	4.11(1), 4.30(2)
78459	143761	0.612	5781	-0.248	-5.097	1, 2, 6, 7, 9	3.892	0.350	4.14(1), 4.36(2)
82588	152391	0.749	5420	0.040	-4.435	1-3, 6, 7	1.996	0.180	4.57(2)
85042	157347	0.680	5623	0.007	-5.017	6, 7, 9, 11	2.018	0.182	4.36(1), 4.50(2)
88945	166435	0.633	5728	0.040	-4.265	6, 7, 9	8.264	0.211	4.44(2)
96185	184499	0.595	5728	-0.634	-5.157	1	5.210	0.469	4.01(1), 4.11(3)
96901	186427	0.661	5702	0.053	-5.050	1, 6, 7, 9	2.557	1.515	4.37(1), 4.35(2)

Note. (a) Surface fluxes F_s are $\times 10^6 \text{ erg cm}^{-2} \text{ s}^{-1}$. (b) Solar F_s values are at cycle 22 maximum and minimum reported by Woods & Rottman (2002). (c) Activity sources are (1) Duncan et al. (1991), (2) Baliunas et al. (1995), (3) Henry et al. (1996), (4) Strassmeier et al. (2000), (5) Tinney et al. (2002), (6) Gray et al. (2003), (7) Wright (2004), (8) Jenkins et al. (2008), (9) Isaacson & Fischer (2010), (10) Arriagada (2011), and (11) Lovis et al. (2011). (d) $\log g$ sources are (1) Cayrel de Strobel et al. (2001), (2) Valenti & Fischer (2005), and (3) Ramírez et al. (2012).

The three criteria for selecting a solar analog are (1) location within $\pm 0.5 \text{ mag}$ of the *Hipparcos* main sequence (HMS; Wright 2004), (2) effective temperature T_e from the Geneva-Copenhagen survey (Holmberg et al. 2009) within $\pm 500 \text{ K}$ of solar, and (3) surface gravity consistent with a dwarf star. For each SW spectrum, the measured flux was integrated over 1250–1910 Å, a wavelength range containing the absorption spectrum of molecular oxygen (Schumann–Runge system; e.g., Wayne 1991). This wavelength-integrated flux was converted to a surface flux F_s using the relation of Oranje et al. (1982) as described in Buccino & Mauas (2008). Distances to these stars range from 3.7 to 32.2 pc, so we make no correction for interstellar extinction. The sample of 33 stars and their properties are listed in Table 1, including the average F_s for each star and its standard deviation used in this study. Table 1 also includes (for most stars) two independent observations of $\log g$, and for all stars $\log g > 4.0$.

Observations of Ca II H+K flux for these stars are taken from Duncan et al. (1991), Baliunas et al. (1995), Henry et al. (1996), Strassmeier et al. (2000), Tinney et al. (2002), Gray et al. (2003), Wright (2004), Jenkins et al. (2008), Isaacson &

Fischer (2010), Arriagada (2011), and Lovis et al. (2011). In all of these reports, except for Lovis et al. (2011), the Ca II H+K fluxes are given in Mt. Wilson S -units (Duncan et al. 1991). The S -units are transformed to $\log R'_{HK}$ by removing the photospheric component using the procedure of Noyes et al. (1984), described in Henry et al. (1996) and Wright (2004).

Metallicity variation influences the photospheric opacity and introduces corresponding variability in the Ca II H+K flux. The $\log R'_{HK}$ values reported by Lovis et al. (2011) have already been corrected to solar metallicity. We adjust all other observations considered here to solar metallicity following Sousa et al. (2008). For this adjustment we preferred spectroscopic metallicity determinations when available. If metallicity observations were available in Cayrel de Strobel et al. (2001), these were averaged. Otherwise, the metallicity was taken from Valenti & Fischer (2005), or if not available there, then from the multi-band photometric estimate in Holmberg et al. (2009).

Metallicity also influences a star's displacement from the HMS. An evolved subgiant can lie on the HMS if it has sufficiently low metallicity. A subgiant has such a contrasting internal structure, age, and rotational history from the Sun that

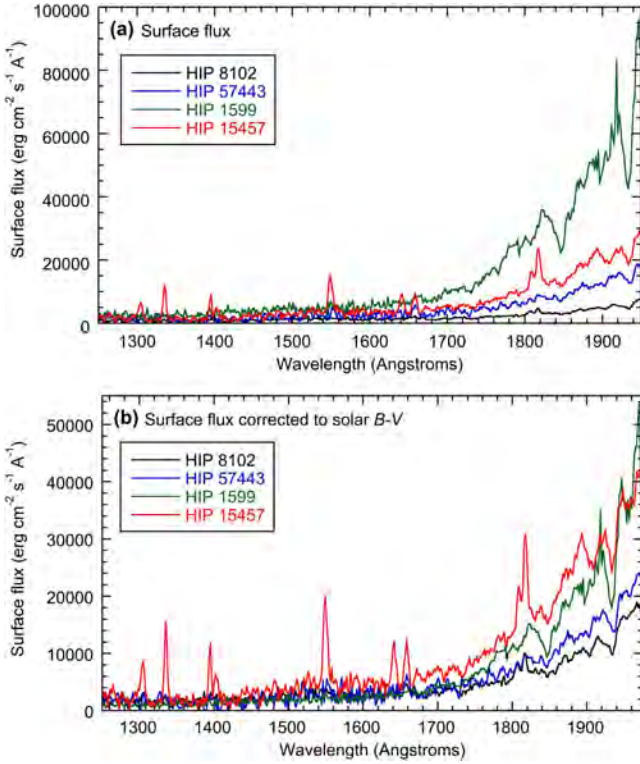


Figure 1. Sample *IUE* SW spectra from four solar analogs with varying activity; (a) spectral surface flux derived from the measurement, and (b) spectral flux corrected to solar $B - V$.

we must take care not to accidentally include definitively evolved stars in our analysis (Jenkins et al. 2008; Saar & Testa 2012). We used the parameterization of Twarog et al. (2009) to check that for any evolved stars that might appear close to the HMS due to significantly non-solar $[\text{Fe}/\text{H}]$. Using this correction we find only two stars (HIP 33719 and HIP 64792) with heights above the HMS of 0.504 and 0.527 magnitudes, respectively. Both are slightly metal-rich stars and may be very slightly evolved, but we retained them in the analysis based on their $\log g$.

Figure 1 shows individual surface flux spectra from four solar analogs: (1) HIP 8102 (τ Cet), a cooler star than the Sun ($B - V = 0.727$) and with steady and low activity (average solar-corrected $\log R'_{\text{HK}} = -5.031$) such that it is widely regarded as a possible grand-minimum star (e.g., Judge et al. 2004; Hall et al. 2009); (2) HIP 57443, a star with near-solar temperature, activity slightly less than mean solar ($B - V = 0.664$ and $\log R'_{\text{HK}} = -4.973$); (3) HIP 15457, a slightly cooler star than the Sun ($B - V = 0.681$) but active ($\log R'_{\text{HK}} = -4.419$); and (4) HIP 1599, a hotter star than the Sun ($B - V = 0.576$) but with activity only slightly greater than mean solar ($\log R'_{\text{HK}} = -4.911$). As expected, the surface flux (left panel of Figure 1) depends very strongly on temperature, with HIP 1599 appearing much brighter than the others. Upon correcting the fluxes to solar temperature (discussed below), the same four objects show differences that correlate with activity. HIP 15457 appears brighter than the others throughout most of the spectral range, and there is a small difference between the grand-minimum candidate HIP 8102 and the solar-activity-range star HIP 57443.

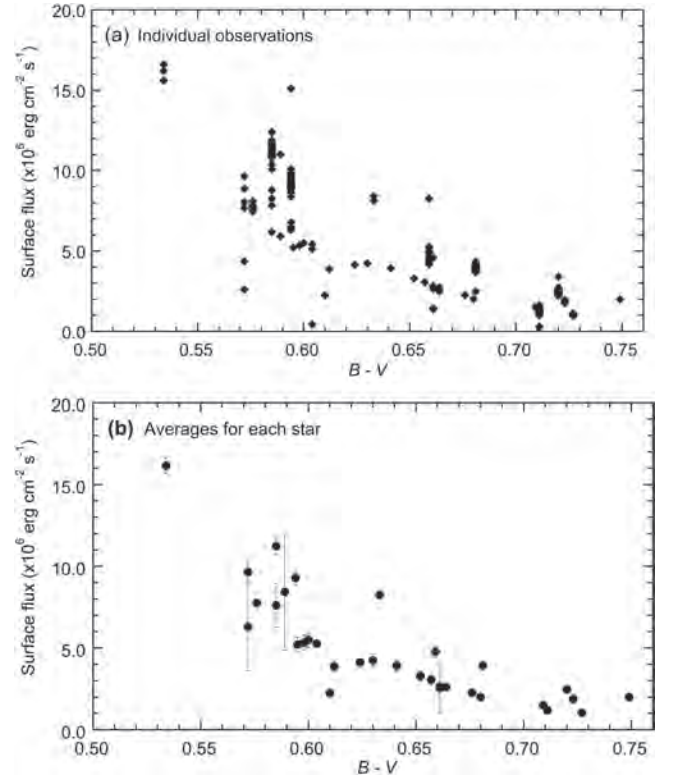


Figure 2. (a) Individual observations (total 211 spectra) of 33 solar analogs integrated over 1250–1910 Å and converted to surface flux plotted vs. color index. (b) Average integrated surface flux F_s for each object, after eight outlying individual observations have been omitted based on the Thompson tau method. Error bars shown in (b) are $\pm 1\sigma$.

3. Analysis

We see a strong relationship between surface flux and $B - V$, similar to what Buccino & Mauas (2008) find for the high-resolution data near the Mg II emission feature. Figure 2(a) shows all individual observations. More outliers appear in this plot than in Figure 2 of Buccino & Mauas, and we reject these outliers on the assumption that they are poorly flux-calibrated observations. To uniformly apply this assumption, we identify these outliers using the modified Thompson tau test and continue iterating on all observations for a given star until either (1) no more outliers are identified, or (2) the standard deviation of the remaining observations is less than 5%, whichever occurs first. Out of 211 *IUE* observations, the modified Thompson tau test rejects only eight. Four surface flux observations are significantly larger than the final mean for the star, and four are smaller. All of the stars from which these individual observations were rejected had 10 or more observations, and no more than 2 observations were rejected per star. Therefore, this initial outlier identification should not bias our final result. The average surface fluxes F_s for each star after these outlier rejections are shown in Figure 2(b).

Our objective is to determine the relationship between F_s and the Ca II H+K chromospheric activity flux $F'_{\text{HK}} = R'_{\text{HK}} \sigma T_e^4$. Plotting these *IUE*-measured F_s averages directly as a function of F'_{HK} (Figure 3(a)) reveals only a weak relationship. To assess the true dependence of surface flux on activity, these average F_s must be normalized to solar temperature. We expect a nonlinear relationship between surface flux and $B - V$, and we tried weighted linear regressions of both $F_s^{1/4}$ and $\log F_s$ against $B - V$ (weighted linear regression being less sensitive to

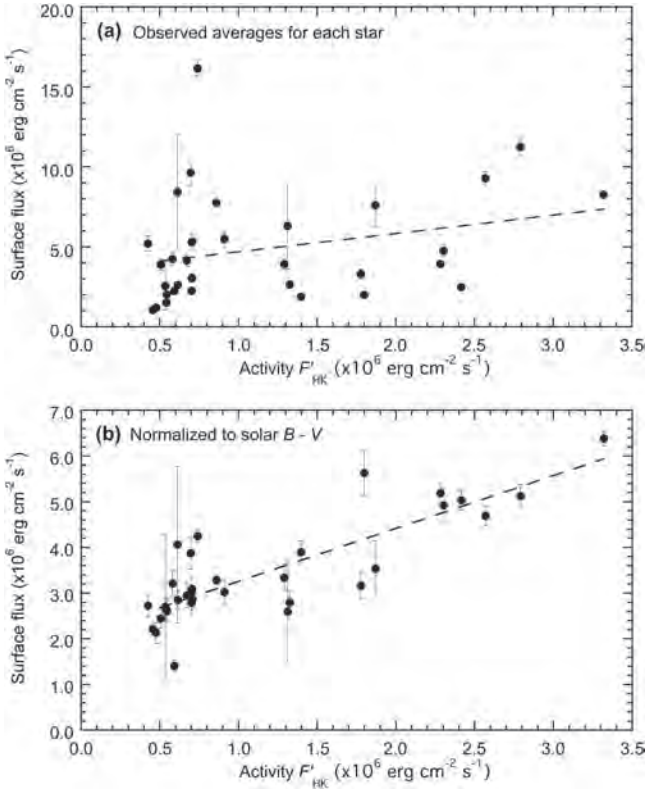


Figure 3. Observed average integrated surface flux over 1250–1910 Å for each solar analog (a) and integrated surface flux normalized to solar $B - V$ (b) plotted vs. activity F'_{HK} .

outliers than ordinary least squares). The regression using $\log F_s$ gives a slightly better correlation. This regression yields slope -4.812 , intercept 9.710 , correlation -0.879 , and $R^2 = 0.773$. After using this regression to normalize the average fluxes to solar $B - V$, we find a strong relationship between these normalized surface fluxes and activity F'_{HK} (Figure 3(b)). In Figure 3(b), a weighted linear regression yields slope 1.2260 , intercept 1.9989×10^6 , correlation 0.859 , and $R^2 = 0.738$.

There is still considerable scatter in Figure 3(b), particularly among the lowest-activity stars. We therefore decided to omit any stars that appear as outliers in a standard statistical test. We apply the Iglewicz & Hoaglin (1993) test for multiple outliers, which with a modified Z-score ≥ 3.5 flags three stars as possible outliers: HIP 37853, HIP 47592, and HIP 51248. HIP 37853 has the lowest metallicity of our sample ($[\text{Fe}/\text{H}] = -0.884$), which might explain its F_s lying well above the regression line. HIP 47592 is the hottest star in our sample ($B - V = 0.534$) and, lying at the extremity of our $B - V$ regression, may not have been completely corrected to solar temperature. HIP 51248 has only one *IUE* observation, and based on Figure 2(a) we might have less confidence on its F_s than those of stars with multiple observations. The remaining 30 average surface fluxes normalized to solar $B - V$ are plotted versus F'_{HK} in Figure 4(a). A weighted linear regression here yields a slope of 1.2130 , intercept 2.0098×10^6 , correlation 0.926 , and $R^2 = 0.857$. Thus, the omission of the three outliers reduced uncertainty but did not significantly alter the slope or intercept of the resulting linear regression.

Metallicity variation should generally affect the relationship between F_s and F'_{HK} , so we tested the sensitivity in our derived

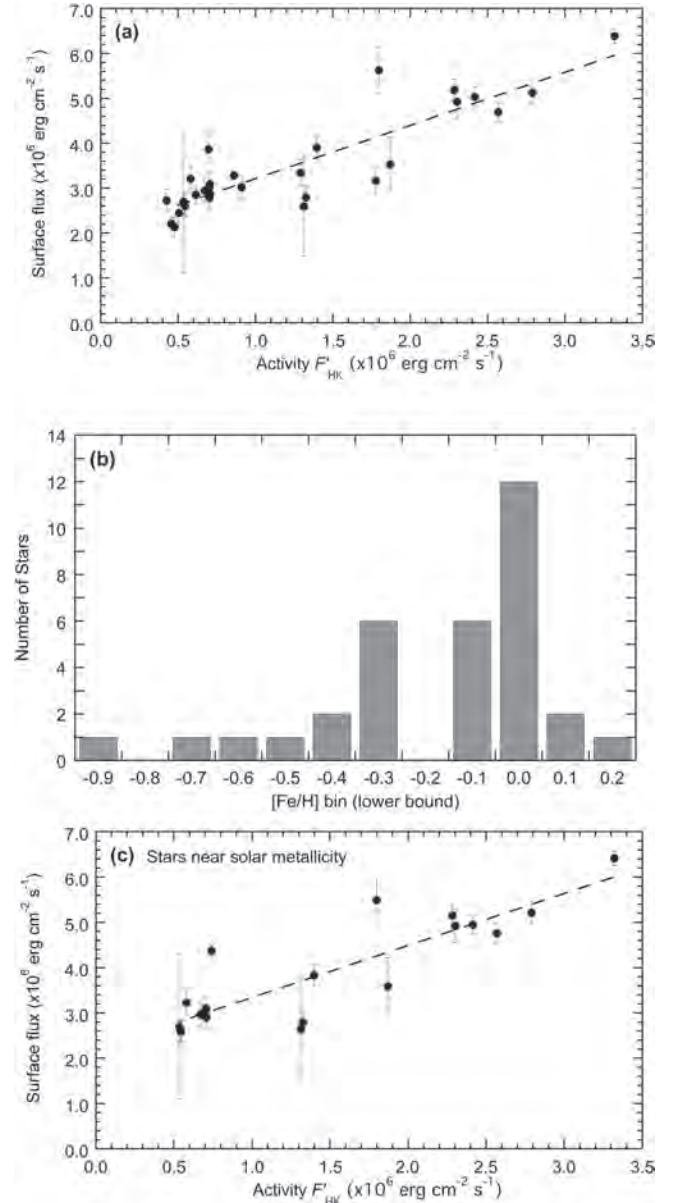


Figure 4. (a) Surface flux integrated over 1250–1910 Å, normalized to solar $B - V$, and with three outliers removed, plotted vs. activity F'_{HK} ; (b) metallicity distribution in the *IUE* sample; and (c) surface flux integrated normalized to solar $B - V$ plotted vs. activity F'_{HK} for the 20 stars with $-0.1 < [\text{Fe}/\text{H}] < +0.2$.

slope and intercept by considering only the stars with metallicity closest to solar. Twenty stars in our sample have $-0.1 < [\text{Fe}/\text{H}] < +0.2$ (Figure 4(b)), and the regression with these stars (Figure 4(c)) yields a slope of 1.1076 , intercept 2.3560×10^6 , correlation 0.884 , and $R^2 = 0.781$. This implies slightly less sensitivity in F_s to F'_{HK} , but is not significantly different than our result in Figure 4(a).

With the linear regression in Figure 4(a) we can estimate the reduction in surface flux under a grand minimum relative to a typical solar minimum. Woods & Rottman (2002) used NASA *Upper Atmosphere Research Satellite* (UARS) observations to evaluate the maximum and minimum spectral solar surface fluxes for cycle 22 for wavelengths shorter than 2000 Å. For the interval 1250–1910 Å, the surface flux at cycle 22 minimum is 9.3% smaller than at maximum. Baliunas et al.

(1995) report Mt. Wilson Ca II H+K observations for the Sun over cycle 22, and from their Figure 1(d) we obtain S -unit values of 0.195 and 0.168 for cycle 22 maximum and minimum, respectively. Following Noyes et al. (1984), these correspond to $\log R'_{HK}$ values of -4.822 and -4.951 , respectively, for solar $B - V = 0.656$. Evaluating the linear regression at these values gives surface fluxes of 3.164×10^6 and $2.867 \times 10^6 \text{ erg cm}^2 \text{ s}^{-1}$, respectively. This difference is 9.4%, consistent with the Woods & Rottman (2002) observations. Schröder et al. (2012) suggest a quiet-Sun value of $S = 0.15$, based on observations of solar activity during cycle 24 minimum on five days in early 2009 when the solar disk was entirely plage-free. With $S = 0.15$ Noyes et al. (1984) give $\log R'_{HK} = -5.065$, and our linear regression of Figure 4 gives a corresponding surface flux $2.669 \times 10^6 \text{ erg cm}^2 \text{ s}^{-1}$. This is 6.9% lower than our estimated value for cycle 22 minimum. The 95% confidence intervals on the slope and intercept of this regression are $1.0210\text{--}1.4050$ and $1.7271\text{--}2.2926 \times 10^6$, respectively. This corresponds to a confidence interval for differences in surface fluxes (a) between solar maximum and solar minimum of 7.7%–11.2%, and (b) between solar minimum and quiet Sun of 5.5%–8.4%. These confidence limits assume that the scatter around the regression line in Figure 4 among the inactive stars is mainly due to flux calibration uncertainty. If we allow the possibility that the scatter represents real stellar variability (probably true for some of the stars), then a wider 95% confidence interval of approximately $\pm 33\%$ applies to any star in the solar activity or inactive range, based on standard confidence estimation for the predicted value in a linear regression model. At present, we cannot resolve which confidence limits apply, not having suitable time series observations of both the activity R'_{HK} and the UV surface flux F_s for all of the stars.

4. Discussion

Reconstructions for UV irradiance from the historical MM to the present-day vary widely. Krivova et al. (2010) estimate a difference between the MM and recent solar minima of 5.1% in the Schumann–Runge continuum (1300–1750 Å) and 1.9% in the Schumann–Runge bands (1750–2000 Å). Lean (2000) reconstructs a difference between MM and mean present-day solar spectral irradiance of $\sim 15\%$ increasing to $\sim 30\%$ as wavelength decreases from ~ 1900 Å to ~ 1300 Å. Our estimate for the interval 1250–1910 Å is 16.3% between quiet Sun and solar maximum, 11.1% between quiet Sun and median present-day solar activity, and 6.9% between quiet Sun and cycle 22 minimum. Our solar analog estimate therefore appears to be intermediate between the Lean (2000) and Krivova et al. (2010) reconstructions.

In contrast, Shapiro et al. (2011) estimate a difference of 26.6% between the MM and recent solar minima in the Schuman–Runge bands (1750–2000 Å). The only way we can construe such a large difference in our *IUE* SW sample is if we consider HIP 8102 (τ Cet), which is the one star in our sample regarded as a likely grand-minimum analog. We estimate its mean activity from the literature (Table 1, corrected to solar metallicity) at $\log R'_{HK} = -5.031$. We have eight SW observations of HIP 8102, none of which were flagged as outliers, and which give an average 1250–1910 Å surface flux (normalized to solar $B - V$) of $2.207 \times 10^6 \text{ erg cm}^{-2} \text{ s}^{-1}$ with a standard deviation of 5.7%. This is 23.0% lower than cycle

22 minimum, and the second lowest value in our sample. It is not clear that we should assert such a large difference based on just one star in our relatively small sample, given that we have no comparable information about the cycling states of most of our other stars in the very low activity or solar-activity ranges. Judge et al. (2004) provide high-resolution spectroscopic evidence in the 1306–1551 Å range that τ Cet may be in a genuine grand-minimum phase. At the same time, τ Cet is metal-poor and so has a shallower convection zone than the Sun for its mass and T_e , and this might influence its activity.

Limitations with this study include the small sample size, unknown quality of the flux calibration, and possibly incomplete metallicity correction of $\log R'_{HK}$ values from the literature. Although published *IUE* SW calibration gives state-of-the-art uncertainties for observations of standard stars early in the *IUE* mission (Bohlin 1986), the scatter in our selected observations led us to reject a few of them as poorly flux-calibrated data. With an early space telescope operating continuously for nearly 18 years, one can naturally expect that not every observation would realize ideal instrument performance. For example, it is possible that some observations did not center the object properly on the aperture. There is a possibility that our somewhat conservative outlier identification procedure for individual spectra did not flag all of the poorly flux-calibrated data (three averages in Figures 2(b) and 3 have large standard deviations: HIP 37583, HIP 64394, and HIP 96901). We note that the solar F_s values on our Figure 4(a) regression line are $\sim 20\%$ larger than the *UARS* measurements (Table 1) reported by Woods & Rottman (2002), although our difference between cycle 22 maximum and minimum is highly consistent with the *UARS* measurements. This is probably a manifestation of the overall flux calibration uncertainty in the *IUE* data. Another limitation with the small sample size is an inability to find many observations that are contemporaneous with the ground-based $\log R'_{HK}$ detections. This introduces uncertainty in the activity values of the most inactive stars, although this uncertainty is probably smaller than those related to the flux calibration. Finally, examination of the metallicity correction in Lovis et al. (2011) and Sousa et al. (2008) reveals that the correction applies only to the bolometric flux term and does not fully correct the R'_{HK} calibration. Based on the metallicity distribution in our sample (Figure 4(b)), we expect this limitation to have minimal influence on our result, although it should be considered when working with a larger sample in future work. Despite these limitations, we find it noteworthy that archival *IUE* data acquired between two and four decades ago for a variety of scientific programs can be compiled here to make a defensible estimate of the change in UV flux between a recent solar cycle minimum and a grand minimum.

This work was supported by California state funds to the Scripps Institution of Oceanography. All of the data presented in this Letter were obtained from the Mikulski Archive for Space Telescopes (MAST). STScI is operated by the Association of Universities for Research in Astronomy, Inc., under NASA contract NAS5-26555. Support for MAST for non-*HST* data is provided by the NASA Office of Space Science via grant NNX09AF08G and by other grants and contracts. We thank the anonymous referee for several insightful suggestions that improved the analysis and manuscript.

ORCID iDs

Carl Melis  <https://orcid.org/0000-0001-9834-7579>

References

- Abreu, J. A., Beer, J., Steinhilber, F., Tobias, S. M., & Weiss, N. O. 2008, *GeoRL*, **35**, L20109
- Arriagada, P. 2011, *ApJ*, **734**, 70
- Baliunas, S. L., Donahue, R. A., Soon, W. H., et al. 1995, *ApJ*, **438**, 269
- Baliunas, S. L., & Jastrow, R. 1990, *Natur*, **348**, 520
- Bohlin, R. C. 1986, *ApJ*, **308**, 1001
- Bohlin, R. C., Harris, A. W., Holm, A. V., & Gry, C. 1990, *ApJS*, **73**, 413
- Bolduc, C., Bourqui, M. S., & Charbonneau, P. 2015, *JASTP*, **132**, 22
- Bolduc, C., Charbonneau, P., Barnabé, R., & Bourqui, M. S. 2014, *SoPh*, **289**, 2891
- Buccino, A. P., & Mauas, P. J. D. 2008, *A&A*, **483**, 903
- Cayrel de Strobel, G., Soubiran, C., & Ralite, N. 2001, *A&A*, **373**, 159
- Curtis, J. L. 2017, *AJ*, **153**, 275
- Duncan, D. K., Vaughan, A. H., Wilson, O. C., et al. 1991, *ApJS*, **76**, 383
- Eddy, J. A. 1976, *Sci*, **192**, 1189
- Feulner, G., & Rahmstorf, S. 2010, *GeoRL*, **37**, L05707
- Gray, L. J., Beer, J., Geller, M., et al. 2010, *RvGeo*, **48**, RG4001
- Gray, R. O., Corbally, C. J., Garrison, R. F., et al. 2003, *AJ*, **126**, 2048
- Hall, J. C., Henry, G. W., Lockwood, G. W., et al. 2009, *AJ*, **138**, 312
- Hall, J. C., & Lockwood, G. W. 2004, *ApJ*, **614**, 942
- Henry, T. J., Soderblom, D. R., Donahue, R. A., et al. 1996, *AJ*, **111**, 439
- Holmberg, J., Nordström, B., & Andersen, J. 2009, *A&A*, **501**, 941
- Iglewicz, B., & Hoaglin, D. C. 1993, in *How to Detect and Handle Outliers*, Vol. 16 of ASCQ Basic References in Quality Control, American Society for Quality Control, ed. E. F. Mykytka (Milwaukee, WI: ASQC Quality Press), 87
- Isaacson, H., & Fischer, D. 2010, *ApJ*, **725**, 875
- Jenkins, J. S., Jones, H. R. A., Pavlenko, Y., et al. 2008, *A&A*, **485**, 571
- Judge, P. G., Saar, S. H., Carlsson, M., & Ayres, T. R. 2004, *ApJ*, **609**, 392
- Krivova, N. A., Vieira, L. E. A., & Solanki, S. K. 2010, *JGR*, **115**, A12112
- Lean, J. 2000, *GeoRL*, **27**, 2425
- Lockwood, M. 2010, *RSPSA*, **466**, 303
- Lovis, C., Dumusque, X., Santos, N. C., et al. 2011, *A&A*, submitted (arXiv:1107.5325v1)
- Lubin, D., Tytler, D., & Kirkman, D. 2012, *ApJL*, **747**, L32
- Maycock, A. C., Ineson, S., Gray, L. J., et al. 2015, *JGR*, **120**, 10943
- Meehl, G. A., Arblaster, J. M., & Marsh, D. R. 2013, *GeoRL*, **40**, 1789
- Noyes, R. W., Hartmann, L. W., Baliunas, S. L., et al. 1984, *ApJ*, **279**, 763
- Oranje, B. G., Zwaan, C., & Middelkoop, F. 1982, *A&A*, **110**, 30
- Orsi, A., Cornuelle, B., & Severinghaus, J. 2012, *GeoRL*, **39**, L09710
- Ramírez, I., Fish, J. R., Lambert, D. L., & Allende Prieto, C. 2012, *ApJ*, **756**, 46
- Saar, S. H., & Testa, P. 2012, in *IAU Symp. 286, Comparative Magnetic Minima: Characterizing Quiet Times in the Sun and Stars*, ed. C. H. Mandrini & D. F. Webb (Cambridge: Cambridge Univ. Press), 335
- Schröder, K.-P., Mittag, M., Pérez Martínez, M. I., et al. 2012, *A&A*, **540**, A130
- Shapiro, A. I., Schmutz, W., Rozanov, E., et al. 2011, *A&A*, **529**, A67
- Song, X., Lubin, D., & Zhang, G. J. 2010, *GeoRL*, **37**, L01703
- Sousa, S. G., Santos, N. C., Mayor, M., et al. 2008, *A&A*, **487**, 373
- Strassmeier, K. G., Washuettl, A., Granzer, Th., et al. 2000, *A&AS*, **142**, 275
- Tinney, C. G., McCarthy, C., Jones, H. R. A., et al. 2002, *MNRAS*, **332**, 759
- Twarog, B. A., Anthony-Twarog, B. J., & Edgington-Giordano, F. 2009, *PASP*, **121**, 1312
- Valenti, J. A., & Fischer, D. A. 2005, *ApJS*, **159**, 141
- Wayne, R. P. 1991, *Chemistry of Atmospheres* (2nd ed.; New York: Oxford Univ. Press), 447
- Woods, T. N., & Rottman, G. J. 2002, in *Atmospheres in the Solar System: Comparative Aeronomy*, Geophysical Monograph, Vol. 130, ed. M. Mendillo, A. Nagy, & J. H. Waite (Washington, DC: American Geophysical Union), 221
- Wright, J. T. 2004, *AJ*, **128**, 1273
- Wright, J. T., Marcy, G. W., Paul Butler, R., et al. 2004, *ApJS*, **152**, 261